Sputtering of water ice

R.A. Baragiola [a,b,*], R.A. Vidal [a,c], W. Svendsen [a,d], J. Schou [a,d],
M. Shi [a], D.A. Bahr [a], C.L. Atteberrry [a]

[a] *Laboratory for Atomic and Surface Physics, University of Virginia, 116 Engineers Way, Charlottesville, VA 22904-4238, USA*
[b] *Università della Calabria and INFM, Arcavacata di Rende (CS) 87036, Italy*
[c] *INTEC, Surface Physics Group, 3000 Santa Fe, Argentina*
[d] *OFD, Risø National Laboratory, DK-4000 Roskilde, Denmark*

Abstract

We present results of a range of experiments of sputtering of water ice together with a guide to the literature. We studied how sputtering depends on the projectile energy and fluence, ice growth temperature, irradiation temperature and external electric fields. We observed luminescence from the decay of H(2p) atoms sputtered by heavy ion impact, but not bulk ice luminescence. Radiolyzed ice does not sputter under 3.7 eV laser irradiation.
© 2002 Elsevier B.V. All rights reserved.

1. Introduction

Irradiation of solids by energetic particles can produce sputtering (ejection) of molecules that leads to the erosion of the surface. The process is characterized by the sputtering yield, Y, the number of molecules (or atoms) ejected per incident projectile. Sputtering may occur in any material as a result of the momentum imparted by the projectile in collisions with target atoms. For this process, termed elastic, or knock-on, sputtering, Y is found to be proportional to the energy deposited by the projectile near the surface when $Y \leqslant 10$, and inversely proportional to the binding energy of the

molecules to the surface [1,2]. Sputtering is fairly well understood for simple metals but not for molecular insulators, like water ice. Experimental studies of sputtering [3–31] and secondary ion emission [32–36] from ice started more than two decades ago when Brown et al. [3] discovered that MeV protons sputtered thin ice films several orders of magnitude faster than expected for elastic sputtering. This meant that sputtering is an important phenomenon on icy satellites and grains subject to irradiation by energetic ions from solar flares and by magnetospheric ions [37]. Brown et al. [5,6] found that Y for fast ions is proportional to the *square* of the electronic energy deposition near the surface. Evidence of this *electronic sputtering* of ice was also present in the observations of emission of ionized water clusters from ice by 80 eV electrons [38].

The conversion of electronic energy into molecular motion in water is still not understood, in spite of many studies. A summary of experimental finding at energies above 10 keV is the following. For ice temperatures lower than about 60–100 K, the total sputtering yield stays essentially constant and increases rapidly at higher temperatures. The main species desorbed at low temperatures are intact water molecules, with near thermal energies. Unlike sputtering of metals, where the most probable energies (E_m) are $\sim 1/2$ the surface binding energies U, for ice E_m is much smaller than $U = 0.45$ eV [39]: it is $\leqslant 1$ meV for H_2O ejected at 12 K by MeV He^+ and Ar^+ and $\leqslant 20$ meV for 50 keV Ar^+ on ice at 25 K [8,11,14].

Mass analysis of the sputtered flux reveals the emission not only of water molecules but also H_2 and O_2 radiation products. Ciavola et al. [7], using 20–100 keV He^+ and Ar^+ impact, found that emission of H_2O and O_2 appears when the ion beam hits the target, but emission of H_2 is delayed and correlates with the square of the electronic energy deposited. For MeV Ne^+ projectiles, H_2 and O_2 was seen to evolve from the ice at a rate that increases with fluence up to a saturation value which depends roughly exponentially on ice temperature [14,26]. The fact that H_2 and O_2 emissions increase also with film thickness at a temperature as low as 7 K but stop when irradiation is interrupted suggests that these molecules are produced at these low temperatures but move significantly only by radiation-enhanced diffusion [26].

The situation is different below 10 keV. Bar-Nun et al. [18] did not detect a fluence dependence in the partial sputtering yields at fluences $>10^{14}$ ions/cm^2. Also using keV ions, de Vries et al. [10,15,16] showed that, at 15–20 K, emission of water predominated over that of fragments and that the energy distribution of O_2 molecules emitted at 20 K by 3 keV Ar^+ peaks at $\leqslant 10$ meV. The contrasting report that water may not be the most abundant species for keV ion impact [18] may result from not considering the much smaller pumping speed for H_2 and O_2 than for water at the cold shield surrounding the target [7,26].

A few studies report that stoichiometry is maintained during ion irradiation, as deduced from Rutherford backscattering (RBS) [3,5,6,12],

or from ejection of H_2 and O_2 molecules in the proportion 2:1 [18]. Still, substantial alterations might occur in the surface layers and not be detectable by RBS, since Auger spectroscopy, which is much more sensitive to the surface, shows changes in the oxygen-KLL Auger spectrum (likely due to oxygen enrichment) after irradiation with large fluences of keV electrons [40].

A recent compilation of sputtering yields by light ions [29] show that, for proton energies below and around the maximum in the electronic stopping cross-section $S_e E = (dE/N\,dx)$, the yield could be approximated by $Y \propto S_e^{1.3}$. Here dE is the differential of electronic energy loss per unit path length dx and N the atomic number density of the target. Analysis of the yield induced by 5 keV/amu H to Ne ions, using theoretical S_e [41], showed $Y \propto S_e^2$ [28]. At lower energies electronic sputtering decreases in importance as elastic sputtering becomes appreciable as evident in the "plateau" that appears in the energy dependence of the yields [18,28]. The quadratic dependence with S_e seen for low temperature ice at high ion energies suggests that two events are needed for electronic sputtering. Mechanisms that have been considered by Brown et al. [8,9] are thermal spikes due to overlapping events along the ionization track of the projectile (which were now shown not to give the quadratic dependence [42]) and Coulomb repulsion between holes.

Fast electrons in electron microscopes, that produce even lower ionization densities than MeV protons, are also able to erode ice [43–46]. The sputtering yield for 100–200 keV electrons appears to be *linear* with the ionization rate [44,45], although this is based only on two data points. That erosion can occur by single excitation events is best evidenced in the photon impact studies of Westley et al. [47] using 10.2 eV photons, which can only produce single excitations or ionizations. They saw a fluence dependence below 80 K for ice grown on polished substrate but the fluence dependence does not appear for ice grown on rough substrates [48], implying photosputtering in single photon events from defect sites.

In this article we show results of several experiments with emphasis on two important questions: the effect of the accumulation of radicals on

sputtering and the relative contribution of inelastic and elastic collisions. We studied the energy dependence of the sputtering yields for a variety of ions at low velocities, the dependence of the yields on fluence and temperature, and the effect of UV laser pulses on ice irradiated with ions.

2. Experimental details

We used a cryogenic target assembly in an ultrahigh vacuum chamber, connected to a mass-analyzed ion accelerator with a base pressure of $\sim 10^{-10}$ Torr [28]. Ice films were grown on a 6-MHz gold-coated quartz-crystal microbalance [39] with a sensitivity of ~ 0.1 monolayer. Luminescence emitted from the ice at 90° to the ion beam (Fig. 1) was analyzed with a vacuum UV-spectrometer using either a photomultiplier or a CCD detector, both with UV–visible conversion coatings. The angle of incidence of the ions was normal for sputtering and 45° for most luminescence studies. We grew amorphous ice films, 150–250 nm thick, by dosing water vapor onto the cooled target crystal. To determine the sputtering yields, we converted the mass loss given by the microbalance to number of water molecules and divided it by the number of incident particles (a small correction is made for the mass of the ions implanted in the ice).
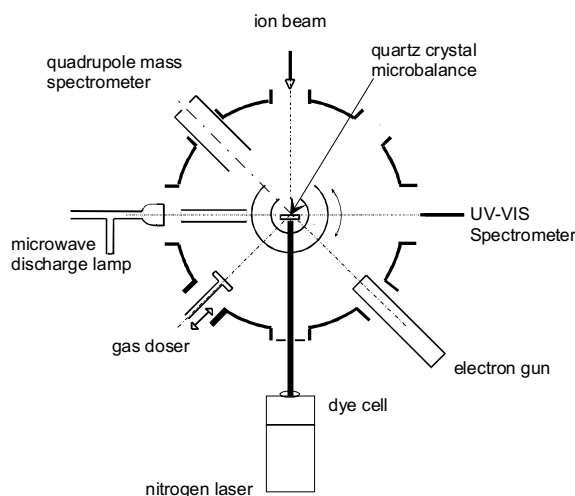
Results were reproducible to $\sim 20\%$ (sample to sample variations), as also noticed by others [3,15]. Yields were insensitive to ion beam current and to the ice growth temperature which gives different crystalline/amorphous content [39]. A related insensitivity to ice properties was found earlier [18,47].

Light from a nitrogen laser operating at the base wavelength 337.1 nm was partly focused to a spot of 0.025 cm^2 on the target through a quartz window. Typically, the laser operated with a ~ 10 Hz repetition rate at an average power of 1.95 mW, which was monitored by the thermal shift of the resonance frequency of the crystal hit in its center by the laser beam. Typically, an 11 Hz shift was seen corresponding to a temperature increase of ~ 0.3 K. We also used a dye cell mounted on the laser to produce visible light with an average power on the target of 0.1 mW at 625 nm. Ice films irradiated for several hours by the laser alone showed no detectable erosion, which is expected in the absence of multi-photon excitations in ice, since the 3.7 eV photon energy is below the absorption threshold of undamaged water, ~ 7.8 eV [49]. In other experiments, films previously irradiated by 0.5–2 keV electrons, 20 keV H^+ or 50 keV Ar^+ ions were subsequently irradiated with the laser to search for effects due to light absorption by radicals or defects.

3. Results and discussion

Temperature dependence: Fig. 2 shows that sputtering yields for 30 keV H^+, He^+, O^+ and Ar^+ are independent of ice temperature up to 60–100 K, where they increase with temperature, similarly to reports for other ions and energies [12,13,21,30]. Brown et al. [6] fitted 0.9 MeV H^+ and 1.5 MeV He^+ data versus temperature T with an expression $Y = Y_0 + Y_1 e^{-E/kT}$, where k is Boltzmann's constant. They reached the conclusion that the two components Y_0 and Y_1 have different S_e dependence: Y_0 being nearly quadratic and Y_1 nearly linear. Using all the data available today, the conclusion is different. Fig. 3 shows that Y_1 is proportional to Y_0 over five orders of magnitude, from the case where $Y_0 \propto S_e$ (electron impact) to
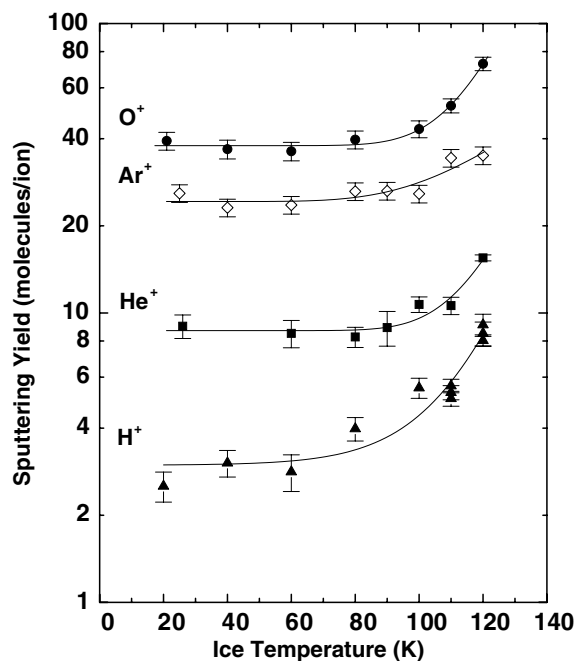

Fig. 1. Experimental setup.

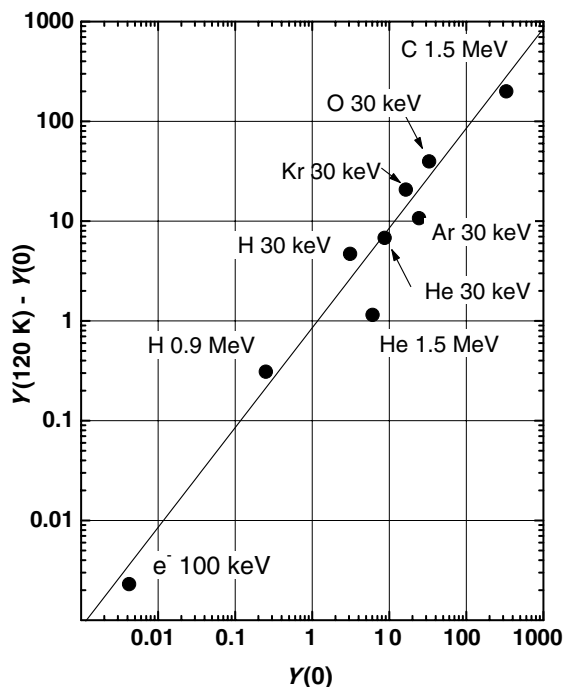Fig. 2. Sputtering yield of ice for 30 keV ions at normal incidence versus temperature.

Fig. 3. The difference in the sputtering yield at 120 K and at <90 K: $Y(120)–Y(0)$, versus $Y(0)$. Data for 30 keV H, He, O and Ar ions: this work; 30 keV Kr [21]. Electron data from [45]. MeV data from [8]. The line is a linear fit, $Y(120 \text{ K}) = 0.85Y(0)$.
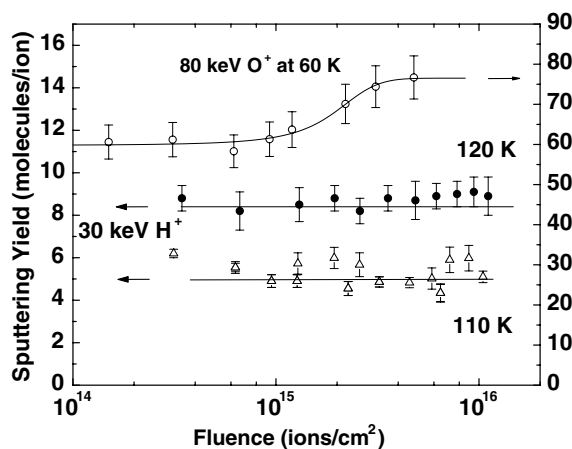

Fig. 4. Sputtering yield of ice versus fluence of bombarding protons and O ions.

the case of MeV ion impact, where $Y_0 \propto S_e^2$. This suggests that Y_0 and Y_1 are related; a possibility is that the effect of temperature is to increase the depth from which molecules are sputtered.

The temperature-dependent component has been attributed to processes involving radicals for which trapping, diffusion and reaction rates depend strongly on temperature [11,13,14,18,44]. The large number of processes involving electrons and multiple neutral, excited and ionized species of H, H_2, O, O_2, H_2O, HO_2 and H_2O_2 makes this problem presently intractable until more information is provided by additional experimental techniques.

Fluence dependence: We studied the effect of ion irradiation fluence on sputtering at 60 K, where Y is independent of temperature and at 110 K, where Y increases rapidly with temperature. Total sputtering yields by protons are independent of fluence up to 10^{16} H$^+$/cm^2 at all temperatures tested in the range 20–120 K, consistent with results for *total* yields by MeV He$^+$ and Ne$^+$ at similar fluences [3,14,26]. Fig. 4 shows results for 110 and 120 K in

the region where the temperature dependence in the yields might suggest a fluence-dependent effect

due to accumulation of radicals. We note that partial yields of H_2 and O_2 do depend on fluence at low temperatures, but at 10 K they are an order of magnitude lower than those of H_2O water; meaning that Y is dominated by emission of water molecules [5,30]. Fig. 4 shows that at 110–120 K, where O_2 and H_2 emission are important, if there is a fluence dependence, it must be at fluences below $\sim 3 \times 10^{14}$ H^+/cm^2, the lowest value we could use. In the case of incident O^+ we see a different behavior, a slight increase in Y with fluence at 60 K (Fig. 4). Due to the large sputtering yield, insufficient amount of implanted oxygen can be trapped in the ice to alter the energy deposition process sufficiently to explain the fluence dependence. Rather, it is possible that the implanted oxygen atoms act as scavengers of electrons or of H and H_2, forming OH, HO_2 and H_2O. Kinetic energy liberated in these and subsequent exothermic reactions involving OH and HO_2 can produce an enhancement in the sputtering yield.

In the MeV experiments by Reimann et al. [14] at 15 K, the fluence dependence of O_2 emission can be understood by assuming that single collisions produce O, but not O_2. To form O_2 by recombination of O, a sufficient O concentration needs to be built up by many projectiles. However, O will most likely react with a water molecule to form H_2O_2 before finding another O atom. An alternative explanation for the fluence dependence of O_2 emission is that O_2 originate from the dissociation of HO_2 and H_2O_2 that accumulate in the ice [50]. We have shown that O_2 buildup in the ice by 80–100 keV protons is small [50], which helped to constrain the source of oxygen in Ganymede, an icy Jovian satellite [51].

Energy dependence: Fig. 5 shows our new values of Y at 60 K versus ion energy, together with our previous results [29]. Ar^+ results of Chrisey et al. [21], not shown in the figure, are much lower than the present values, as noticed previously [28]. Anomalous low yields may result from very rough surfaces [52] caused by the large fluences required by Chrisey's technique. This effect was also noted by Evatt [4] and by Rocard et al. [19], who reported a significant decrease in Y after about 200 nm of their ice samples were sputtered with 15–30 keV ions. Evidence for unusual roughening of ice
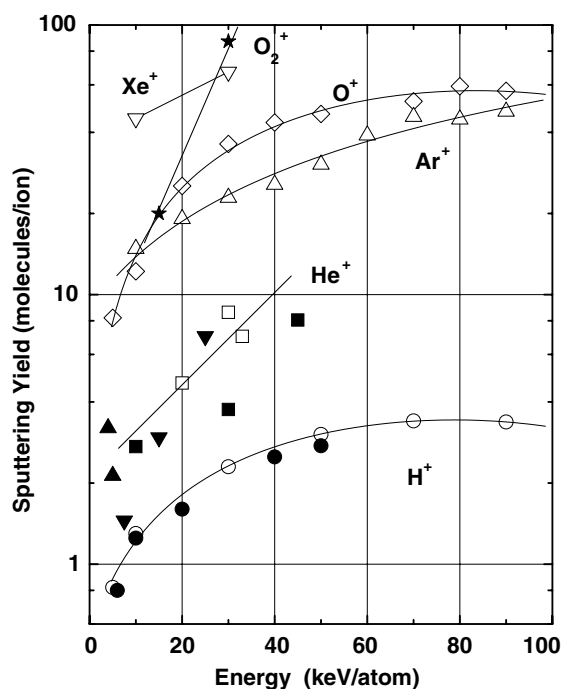

Fig. 5. Sputtering yield of ice at 60 K versus projectile energy. This work: open symbols. Brown et al. [5]: ●: H; ■: He. Christiansen et al. [23]: ▲: He. Rocard et al. [19]: ▼, H, He.

by ion bombardment comes from electron microscopy [17] and RBS [26,53] studies.

Molecular effect in sputtering: We also measured Y for molecular O_2^+ at 30 and 60 keV and found them to be 2 and 4.3 times that for O^+ incident at the same velocity. Although Y for this projectile pair is additive at 15 keV/atom, it is not at 30 keV/atom. This indicates that yields are not additive at higher energies and do not scale like the square of the energy deposited near the surface as it does for sputtering with H^+ and H_2^+ ions [8,19].

Effect of electric fields on sputtering: When an ice film is bombarded by ions, electron–hole pairs are created along the projectile ionization track. If the electrons are extracted, unbalanced holes remain. We asked if the repulsion force between unbalanced holes would be sufficient to cause sputtering or if, alternatively, electron removal might lead to a reduced sputtering yield, as for Ar [54], by inhibiting recombination into excited states. We measured Y using 30 keV He^+ changing the bias of an anode surrounding the target from

−300 to +300 V, where electrons are extracted from the ice, and found no change in Y within ±10%.

Ionoluminescence: Strong light emission peaking at ∼121.6 nm, the hydrogen Lyman-α wavelength, was seen from the surface during bombardment by 30 keV Ar, Kr and Xe ions at 45° incidence. We observed Lyman-α; the width of the line was ∼8 nm (with a 2 nm resolution) and a weak signal due to sputtered excited OH at 306 nm. Lyman-α luminescence does not depend on film thickness over a wide range, suggesting a surface collision process, since the escape depth of Lyman-α photons in ice is 39 nm (26 μm^{-1} absorption coefficient [49]). Thus, the strong light emission that we observe comes from sputtered excited H(2p) decaying in vacuum close to the surface (the lifetime is a few ns). As a test, we deposited a 10^{17} mol/cm² of solid CO_2 on top of the water ice which was then bombarded by 50 keV Ar⁺ ions. This layer was thin enough to allow the ions to deposit a significant fraction of their energy in the ice, and to allow bulk luminescence to partially escape, but thick enough to prevent significant sputtering of water molecules. We detected no Lyman-α until the overlayer was sputtered away, showing again that the H(2p) comes from surface collision processes.

Heavy projectiles can transfer momentum to H(2p) and eject it from the solid, or to an excited water molecule that is ejected and breaks up outside the surface producing H(2p). In both cases, the excited atom can be ejected and survive quenching by radiationless transitions in the solid. The Lyman-α line is significantly broader than expected from the Doppler effect due to a distribution of H(2p) velocities; the additional broadening mechanism may be an Auger deexcitation process involving the surface [55]. A much weaker H(2p) ejection by H⁺ impact may result from purely electronic processes involving repulsive excited states, as seen in the ejection of H(2s) atoms with energies of a few eV by incident 17–50 eV electrons which cannot break bonds by direct momentum transfer [56,57].

The luminescence signal is constant with temperature, in strong contrast to the variation of Y in the same region. This behavior is expected if luminescence comes from excitations accompanying knock-on sputtering, which should not depend on temperature in the conditions of our experiment. The temperature independence also indicates that thermally activated processes, such as diffusion of excitations, are not significant for luminescence. Fig. 6 shows that the energy dependence of the luminescence signal is stronger than that of Y. This is expected from a knock-on process that also involves an electronic excitation as occurs, e.g. in inner shell excitation by slow ions [55].

We searched extensively for but did not observe bulk luminescence, with incidence angles from 0 to 70°, even when using large 5 μA/cm² 100 keV H⁺ beams, two to three orders of magnitude more intense than used in sputtering measurements. The negative result contrasts with multiple reports of bulk ice luminescence by Quickenden et al. [58–60] which may be caused by impurities co-deposited at 10^{-6} Torr since these authors also observed luminescence with 260 nm photons, which fall in the band gap of ice.
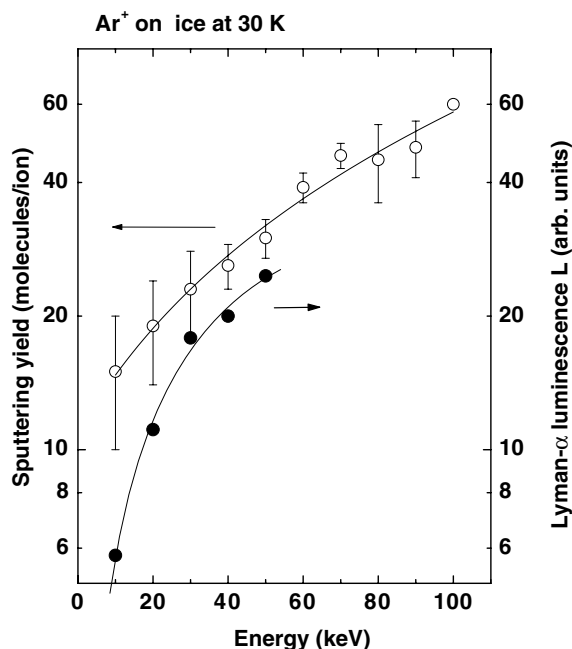

Fig. 6. Energy dependence of the Lyman-α luminescence efficiency and the sputtering yield of ice bombarded by Ar⁺ ions at 30 K.

Laser irradiation of radiolyzed ice: We performed experiments aimed at studying the concentration of species produced by irradiation with ions and electrons. The storage of radiation products in ice has been demonstrated by the emission of HO_2, H_2O_2 and O_2 in thermal desorption experiments on previously irradiated ice [47,50]. Recent photochemistry studies [61] using Lyman-α at 10 K show that the concentration of OH first increases with photon fluence but then declines above a fluence of $\sim 10^{17}$ photons/cm^2 where the formation of HO_2 and H_2O_2 increases in importance. Virgin ice starts absorbing light at ~7.3 eV [49] and therefore it is transparent to the 3.7 eV photons from the laser. Hence, no sputtering can result at the photon intensities used in our experiments, where multiphoton absorption is insignificant. The experiments tested if desorption could be triggered by light absorption by species such as OH and HO_2 or trapped electrons produced by prior ion irradiation. Fig. 7 depicts the effect of laser irradiation on 100 nm water ice. First, it shows the thermal effect on the quartz crystal during an hour. In this particular run, the ice was bombarded to a fluence of 4.8×10^{20} photons/cm^2. No sputtering appears above the sensitivity of 0.5 monolayers. Laser irradiation of ice pre-bombarded with 1.6×10^{16} ions/cm^2 H$^+$ at 20 keV also did not lead to detectable sputtering

(sputtering by H$^+$ is seen in the slope of the crystal frequency versus time in Fig. 7). The effect of laser irradiation on the ion-irradiated sample is similar to that seen before ion irradiation and explained again by laser heating. This means that ion irradiation did not produce a sufficient number of long-lived radicals, other species or defects that would produce photosputtering from the nitrogen laser above the detection limit. Other combinations of pre-bombardment by ions, electrons or 10.2 eV photons also did not lead to measurable photosputtering with the laser.

In other experiments, we irradiated ice with light ions at 7–8 K and high fluences to enhance the accumulation of radicals. We did not observe the oscillations in desorption reported by Hudson and Moore [62], for a range of experimental conditions (ice thickness between 0.5 and 10 μm, 50 keV H$^+$, H$_2^+$ or He$^+$, and fluences up to 10^{15} ions/cm^2). Further irradiation of these irradiated ices with the nitrogen laser did not result in sputtering above 6×10^{-7} H$_2$O/photon. We note that Leto et al. [63] also could not observe pressure oscillations for 3 keV He$^+$ bombardment of ice films, several tens of nm thick, at 10 K.

Stopping power dependence: As expected from previous measurements [28,64], we find that Y is non-linear on S_e. Fig. 8 shows a summary of Y versus S_e derived from measurements [65] for H$^+$ and from theory [41] for heavy ions. An estimate of the linear yield in ice is obtained using Y produced by 100–200 keV electrons [45] and tabulated S_e [66], taking into account the enhanced energy deposition near the surface by backscattered electrons [67]. The derived yield is

$$Y_1 = (S_e/440) \ (\text{molecule/eV } \text{Å}^2),$$

Y_1 is plotted in Fig. 8 as a line labeled "electron": (the experimental values are too small to appear in the graph). It lies above the highest energy data point of the MeV proton experiments probably due to experimental uncertainties since there is no apparent reason why electrons would sputter more efficiently than fast protons at the same value of deposited energy. We note that further evidence for sputtering caused by single events comes from experiments with incident 5–120 eV electrons
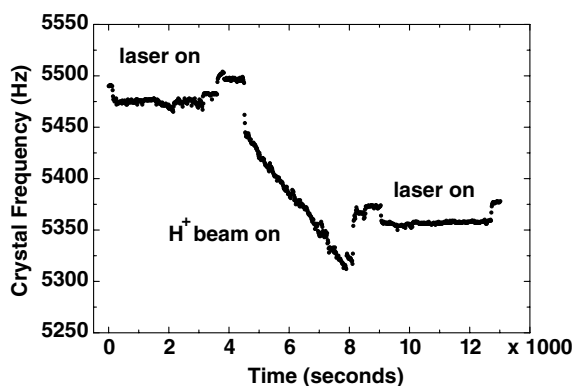

Fig. 7. Frequency change of the quartz crystal with a 100 nm ice film at 35 K versus time showing the effect of irradiation with a 140 nA beam of 20 keV H$^+$, and with 337.1 nm laser light.
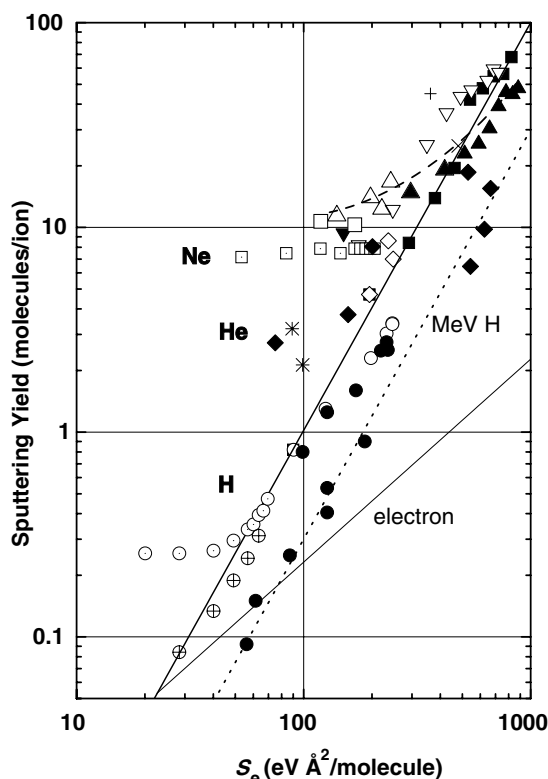
Fig. 8. Sputtering yields of ice versus the electronic stopping cross-section S_e. This work: ○: H, ◇: He, ▽: O, ▲: Ar, +: Xe. Shi et al. [28]: ■: H through Ne. Brown et al. [5]: ●: H, ◆: He. Bar Nun et al. [18]: ⊙: H, ▢: Ne. Christiansen et al. [23]: ∗: He, ▼: N, □: Ne, ▽: Ar. Spinella et al. [27]: ×: He. ⊕: is the sputtering yield for H of Bar Nun et al. [18] minus the estimated elastic contribution. The thick solid line is a fit to the Z-dependence of [28]. The dotted line labeled "MeV H" is a fit to the data of [5]. The line labeled "electron" is an extrapolation to the high-energy electron impact data [45].

(e.g. [38,56,57]). Since electrons with these energies are generated in the ice by fast ions at a rate that is linear with S_e, electron-induced processes should give a linear contribution to the sputtering yield for ions.

For MeV protons, $Y \propto S_e^2$ which, as mentioned above, is not yet understood but is likely connected with the overlap of two excitation events [22]. This *quadratic* yield can be expressed, based on the MeV H⁺ data as

$$Y_2 = (S_e/183 \text{ molecule/eV} \text{\AA}^2)^2.$$

Deviations from the quadratic dependence at low velocities may result from a number of effects: the incident charge of the ion is not equal to the equilibrium value, target ionization can be caused by electron capture collisions, and there may be synergism between electronic and elastic collision processes. A further effect is the occurrence of collision spikes [2,42], a dense collision cascade where most species are in motion and where the usual concept of surface binding energy of a single molecule may not be applicable.

The contribution to sputtering due to elastic collisions, Y_n, is usually assumed to be additive to inelastic sputtering: $Y = Y_n + Y_1 + Y_2$. Christiansen et al. [23] analyzed it by comparing measurements with results from Sigmund's theory [1] for the sputtering of *monoatomic* solids:

$$Y_n = (3/4\pi^2)\alpha S_n/(C_0 U),$$

where S_n is the elastic ("nuclear") stopping cross-section; α a tabulated function of the mass ratio in a collision; C_0 an effective cross-section for low energy recoils; and $U = 0.45$ eV. Christiansen et al. [23] did not specify the value of C_0 they used for the calculation but concluded from the agreement between the measured and calculated sputtering yields that elastic collisions are the major contribution to sputtering by low keV ions. Chrisey et al. [21] noted that the straightforward application of Sigmund's theory was not appropriate for molecular targets and used a factor of $1/3$ to convert the molecular stopping cross-section to an atomic value:

$$Y_n = 0.014 \text{ \AA}^{-2}\alpha S_n/U,$$

where S_n is the stopping cross-section per water molecule computed as the sum of atomic stopping cross-sections. We obtain the proportionality factor between Y_n and S_n from experiments using compiled values of S_n [68]. We have used results of [18] by adjusting the Y measured at oblique incidence to normal incidence by calculating the angular dependence of the energy deposited near the surface by the incident ions [68]. Table 1 shows that $Y_n/(\alpha S_n/U)$ agrees with the estimate of Chrisey et al. [21], to better than a factor of two, which is reasonable given the approximations in the analytical sputtering theory. At high values of S_n

Table 1
Sputtering yields due to nuclear collisions and nuclear stopping cross-section for low energy ions in ice

Ion	Energy (keV)	S_n (eV Å^2/mol)	αS_n (eV Å^2/mol)	Y_n	$Y_n/(\alpha S_n U)$ (Å^{-2})
H	0.25	16	11–16	0.26	0.011
Ne	2–6	600	147	7.9	0.024
Ar	10	1200	240	10	0.019

other factors occur [30]. Other aspects that may still be considered are the mass mismatch between O and H, dissociation events, and the fraction of the elastic deposited energy that goes into vibrations.

4. Conclusions

We can summarize what is known about sputtering of ice from these and previous experiments as follows:

(1) The total sputtering yield is constant below 60–100 K and then rises strongly due to the temperature-dependent H_2 and O_2 emission. (The yield of sputtered water molecules is constant up to 140 K.)

(2) The total sputtering yield is independent of thickness above 2 nm but the partial H_2 and O_2 yields increase with thickness for ion impact.

(3) No fluence dependence of the total sputtering yield appears except a weak one for keV oxygen ion bombardment. The yield of H_2 and O_2 depends on fluence at low temperatures.

(4) Sputtering can occur by elastic or inelastic (electronic) processes. Electronic sputtering can occur by single events as seen in photon and electron impact at low and very high energies. For fast ions, the sputtering yield is roughly proportional to S_e^2.

(5) Luminescence from ion-bombarded water ice occurs only for heavy projectiles and originates from decay of sputtered excited H(2p) atoms. Bulk luminescence is insignificant.

(6) No laser sputtering was observed with sub-bandgap light on ice that was radiolyzed by different combinations of keV ions, electrons and Lyman-α photons.

References

[1] P. Sigmund, Phys. Rev. 184 (1969) 383.
[2] P. Sigmund, in: I.R. Behrisch (Ed.), Sputtering by Particle Bombardment, Springer Verlag, Berlin, 1981 (Chapter 2).
[3] W.L. Brown, L.J. Lanzerotti, J.M. Poate, W.M. Augustyniak, Phys. Rev. Lett. 40 (1978) 1027.
[4] R.W. Evatt, M. Sc. Thesis, University of Virginia, 1980.
[5] W.L. Brown, W.M. Augustyniak, E. Brody, B. Cooper, L.J. Lanzerotti, A. Ramirez, R. Evatt, R.E. Johnson, Nucl. Instr. and Meth. 170 (1980) 321.
[6] W.L. Brown, W.M. Augustyniak, L.J. Lanzerotti, R.E. Johnson, R. Evatt, Phys. Rev. Lett. 45 (1980) 1632.
[7] G. Ciavola, G. Foti, L. Torrisi, V. Pirronello, G. Strazzulla, Radiat. Eff. 65 (1982) 167.
[8] W.L. Brown, W.M. Augustyniak, E.H. Simmons, K.J. Marcantonio, L.J. Lanzerotti, R.E. Johnson, J.W. Boring, C.T. Reimann, G. Foti, V. Pirronello, Nucl. Instr. and Meth. 198 (1982) 1.
[9] R.E. Johnson, W.L. Brown, Nucl. Instr. and Meth 198 (1982) 103.
[10] R.A. Haring, A. Haring, F.S. Klein, A.C. Kummel, A.E. de Vries, Nucl. Instr. and Meth. 211 (1983) 529.
[11] J.W. Boring, R.E. Johnson, C.T. Reimann, J.W. Garret, W.L. Brown, K.J. Marcantonio, Nucl. Instr. and Meth. 218 (1983) 707.
[12] B.H. Cooper, T.A. Tombrello, Radiat. Eff. 80 (1984) 203.
[13] W.L. Brown, W.M. Augustyniak, K.J. Marcantonio, E.H. Simmons, J.W. Boring, R.E. Johnson, C.T. Reimann, Nucl. Instr. and Meth. B 1 (1984) 307.

[14] C.T. Reimann, J.W. Boring, R.E. Johnson, J.W. Garrett, K.R. Farmer, W.L. Brown, K.J. Marcantonio, W.M. Augustyniak, Surf. Sci. 147 (1984) 227.

[15] R.A. Haring, R. Pedrys, D.J. Oostra, A. Haring, A.E. de Vries, Nucl. Instr. and Meth. B 5 (1984) 476.

[16] A.E. de Vries, R.A. Haring, A. Haring, F.S. Klein, A.C. Kummel, F.W. Saris, J. Phys. Chem. 88 (1984) 4510.

[17] R.E. Johnson, L.A. Barton, J.W. Boring, W.A. Jesser, W.L. Brown, L.J. Lanzerotti, in: J. Klinger, D. Benest, A. Dollfus, R. Smoluchowski (Eds.), Ices in the Solar System, Reidel Publ, Norwell, MA, 1985, p. 301.

[18] A. Bar-Nun, G. Herman, M.L. Rappaport, Yu. Mekler, Surf. Sci. 150 (1985);
A. Bar-Nun, G. Herman, M.L. Rappaport, Yu. Mekler, in: J. Klinger, D. Benest, A. Dollfus, R. Smoluchowski (Eds.), Ices in the Solar System, Reidel Publ, Norwell, MA, 1985, p. 287.

[19] F. Rocard, J. Bénit, J.-P. Bibring, D. Ledu, R. Meunier, Radiat. Eff. 99 (1986) 97.

[20] J. Benit, J.-P. Bibring, S. Della Negra, Y. Le Beyeq, F. Rocard, Radiat. Eff. 99 (1986) 105.

[21] D.B. Chrisey, J.W. Boring, J.A. Phipps, R.E. Johnson, W.L. Brown, Nucl. Instr. and Meth. B 13 (1986) 360.

[22] W.L. Brown, L.J. Lanzerotti, K.J. Marcantonio, R.E. Johnson, C.T. Reimann, Nucl. Instr. and Meth. B 14 (1986) 392.

[23] J.W. Christiansen, D. Delli Carpini, I.S.T. Tsong, Nucl. Instr. and Meth. B 15 (1986) 218.

[24] J.W. Christiansen, I.S.T. Tsong, S.H. Liu, J. Chem. Phys. 86 (1987) 4701.

[25] J. Benit, These Dr. Sc., Univ. Paris-Sud, Orsay, France, 1987.

[26] J. Benit, W.L. Brown, Nucl. Instr. and Meth. B 46 (1990) 448.

[27] F. Spinella, G.A. Baratta, G. Strazzulla, I. Torrisi, Radiat. Eff. Def. Solids 115 (1991) 307.

[28] M. Shi, D.E. Grosjean, J. Schou, R.A. Baragiola, Nucl. Instr. and Meth. B 96 (1995) 524.

[29] M. Shi, R.A. Baragiola, D.E. Grosjean, R.E. Johnson, S. Jurac, J. Schou, J. Geophys. Res. 100 (1995) 26, 387.

[30] R. Pedrys, F. Krok, P. Leskiewicz, J. Schou, U. Podschaske, B. Cleff, Nucl. Instr. and Meth. B 164–165 (2000) 861.

[31] R.A. Baragiola, C.L. Atteberry, C.A. Dukes, M. Famá, B.D. Teolis, Nucl. Instr. and Meth. 193 (2002) 720.

[32] E.N. Nikolaev, G.D. Tantsyrev, V.A. Saraev, Sov. Phys. Tech. Phys. 23 (1978) 241.

[33] G.M. Lancaster, F. Honda, Y. Fukuda, J.W. Rabalais, Int. J. Mass Spectrom. Ion Phys. 29 (1979) 199;
J. Am. Chem. Soc. 101 (1979) 1951.

[34] J. Benit, These Dr. Sc., Univ. Paris-Sud, Orsay, France, 1987.

[35] R.F. Magnera, D.E. David, J. Michl, Chem. Phys. Lett. 182 (1991) 363.

[36] T. Matsuo, T. Tonuma, H. Kumagai, H. Shibata, H. Tawara, J. Chem. Phys. 101 (1994) 5356.

[37] L.J. Lanzerotti, W.L. Brown, J.M. Poate, W.M. Augustyniak, Geophys. Res. Lett. 5 (1978) 155.

[38] G.R. Floyd, R.H. Prince, Nature (Phys. Sci.) 240 (1972) 11.

[39] N.J. Sack, R.A. Baragiola, Phys. Rev. B 48 (1993) 9973.

[40] P.H. Holloway, T.E. Madey, C.T. Campbell, R.R. Rye, J.E. Houston, Surf. Sci. 88 (1979) 121.

[41] B.S. Yarlagadda, J.E. Robinson, W. Brandt, Phys. Rev. B 17 (1978) 3473.

[42] E. Bringa, R.E. Johnson, Phys. Rev. Lett. 88 (2002) 165501.

[43] Y. Talmon, H.T. Davis, L.E. Scriven, E.L. Thomas, J. Microsc. 117 (1979) 321.

[44] H.G. Heide, Ultramicroscopy 7 (1982) 299.

[45] H.G. Heide, Ultramicroscopy 14 (1984) 271.

[46] H.G. Heide, E. Zeitler, Ultramicroscopy 16 (1985) 151.

[47] M.S. Westley, R.A. Baragiola, R.E. Johnson, G.A. Baratta, Nature 373 (1995) 405;
Planet. Space Sci. 43, 1311.

[48] D.A. Bahr, M. Famá, R.A. Vidal, J. Schou, R.A. Baragiola, to be published.

[49] S.G. Warren, Appl. Opt. 23 (1984) 1206.

[50] D.A. Bahr, M.A. Famá, R.A. Vidal, R.A. Baragiola, J. Geophys. Res. E 106 (2001) 33, 285.

[51] R.A. Vidal, D.A. Bahr, R.A. Baragiola, M. Peters, Science 276 (1997) 1839.

[52] B. Hapke, Icarus 66 (1986) 270.

[53] L.J. Lanzerotti, W.L. Brown, R.E. Johnson, Nucl. Instr. and Meth. B 14 (1986) 373.

[54] D.E. Grosjean, R.A. Baragiola, W.L. Brown, Phys. Rev. Lett. 74 (1995) 1474.

[55] R.A. Baragiola, in: J.W. Rabalais (Ed.), Low Energy Ion-Surface Interactions, Wiley, NY, 1994 (Chapter 4).

[56] R.H. Stulen, J. Vac. Sci. Technol. A 1 (1983) 1163.

[57] G.A. Kimmel, T.M. Orlando, P. Cloutier, L. Sanche, J. Phys. Chem. B 101 (1997) 6301.

[58] D. Lennon, T.I. Quickenden, C.G. Freeman, Chem. Phys. Lett. 201 (1993) 120.

[59] A.J. Matich, M.G. Bakker, D. Lennon, T.I. Quickenden, C.G. Freeman, J. Phys. Chem. 97 (1993) 10539.

[60] T.I. Quickenden, T.A. Green, D. Lennon, J. Phys. Chem. 100 (1996) 16801.

[61] P.A. Gerakines, W.A. Schutte, P. Ehrenfreund, Astron. Astrophys. 312 (1996) 289.

[62] R.L. Hudson, M.H. Moore, J. Phys. Chem. 96 (1992) 6500.

[63] G. Leto, M.E. Palumbo, G. Strazzulla, Nucl. Instr. and Meth. B 116 (1996) 49.

[64] R.E. Johnson, J. Schou, Mat. Fys. Medd. Kgl. Vid. Selsk. 43 (1993) 403.

[65] P. Bauer, W. Käferböck, V. Necas, Nucl. Instr. and Meth. B 93 (1994) 132.

[66] IUCRU, Stopping powers and ranges of electrons and positrons. International Commission on Radiation Units and Measurements Rep. 37 (1984) 206.

[67] L.V. Spencer, Energy Dissipation by Fast Electrons. National Bureau of Standards Monogr. 1 (1959) 13.

[68] J.F. Ziegler, TRIM-96, IBM Corporation, Yorktown Heights, NY, 1996.